Rev. Roum. Sci. Techn.– Électrotechn. et Énerg.
Vol. **69**, *4*, pp. 389–394, Bucarest, 2024

COMBINED FIRST AND SECOND-ORDER SLIDING MODE CONTROL OF INDUCTION MOTOR

HADDA BENDERRADJI, SAMIRA BENAICHA, YAHIA LAAMARI

Keywords: Induction motor control; Sliding mode control; Modelling; Hybrid control; Chattering phenomenon.

This paper uses hybrid sliding mode control to solve an output feedback tracking problem for the induction motor (IM). The main idea of this approach lies in the design of a law that ensures a smooth transition between two sliding regimes based on the choice of two sliding surfaces, one being linked to the other. The control is a combination of first and second-order sliding modes. The proposed approach controls the speed and rotor flux amplitude of the induction motor and guarantees the stability of the decoupled speed and rotor flux by using a Lyapunov method. The hybrid sliding mode algorithm provides robustness despite external disturbances and parameter variations. The controller has been implemented on an experimental setup, and results are presented to confirm the proposed method's effectiveness, robustness, and good performance.

1. INTRODUCTION

Induction motors (IM) have been widely employed in industrial applications. With the development of power electronics technology, several control approaches, including field-oriented control (FOC) and variable structure control, have been used to regulate the IM in high-performance systems [1–5].

The sliding mode (SM) approach has received worldwide recognition and much attention in recent years for controlling induction machines. Ideal sliding mode control (SMC) is a unique nonlinear regulation approach with a particularly dynamic performance for IM, such as high resilience, quick response, and easy implementation in theory and practice—moreover, the most significant property of its robustness, fast dynamic response and insensitivity to parameter variations. We can see in [1] the basic concepts and principles of sliding-mode control of electric drives, and some aspects of the implementation are illustrated in [2].

However, the SMC suffers from chattering, which is a significant drawback. The chattering problem is due to the SMC's discontinuous nature, the control algorithm period, and the maximum power inverter switching frequency [1].

Several searches have proposed integral sliding mode control to ensure asymptotic tracking with zero steady-state error and reduce chattering [6–9]. For instance, in [6,7], the sliding control law in the form of an integral switching surface has been defined to improve the high performance of an IM. In [8], the proportional-integral (PI) speed controller of conventional indirect field-oriented control is replaced with a sliding mode controller, in which the hyperbolic tangent function is used as a switching function aiming for a reduction in the chattering effect. Moreover, in [9], an integral sliding mode controller with a new anti-windup mechanism is used to speed up IM.

In [10], the authors utilized the integral sliding mode technique to design an observer for the IM's predictive stator current control algorithm.

Some authors have used other methods, such as the saturation function, variable-bandwidth filter [11], and boundary-layer solutions [12]. However, integral action can achieve zero steady-state error. Due to the nonlinearity of the IM, such controllers do not handle well and lead to deterioration of the system's transient response.

Furthermore, in [13,14], the authors suggested an SMC with other advanced control methods. [13] proposes a combination of the backstepping control and the synergetic-sliding mode controller. This control relies on combining backstepping and synergetic SMC advantages to control the IM speed. Moreover, in [14], the hybrid control is designed to regulate the speed of IM and to reduce chattering by embedding a fuzzy logic control into the sliding mode control. It is essential to consider that using SMC in combination with other control methods increases the regulator's complexity, which contrasts with the simplicity of SMC.

Concerning chattering reduction, a novel class of SMC algorithm called the second-order sliding mode (2-SMC) algorithm has been developed [15-17]. This approach allows finite-time convergence to zero of the sliding manifolds and their derivatives. Several studies have used this approach to achieve high performance and robust control of IM and reduce the chattering phenomenon [18–21]. For instance, in [18], authors present a novel cascade proportional-integral (PI) continuous second-order sliding mode control for IM using two loops; the inner-loop SMC controls the current dynamics of the motor, while the outer loop is the PI controls speed.

[19] propose the input-output feedback linearization for the exact decoupling of electromagnetic torque and rotor flux using a fractional-order sliding mode controller for speed control. In [20], a super twisting sliding mode algorithm is employed for direct torque and flux control for speed control of IM and reducing the chattering phenomenon. Moreover, [21] presents a second-order terminal sliding-mode speed controller with a nonlinear control gain using the anti-windup mechanism. However, at some operating points, these solutions cause instability.

The subject of this paper is concerned with the application of hybrid SMC for vector-controlled IM speed and rotor flux. The control idea is based on employing two sliding surfaces, and the first surface's convergence depends on the second's convergence. A first- and second-order SMC combination is proposed to achieve input-output decoupling between speed and rotor flux and ensure tracking with high dynamic performances. The experiment results are presented and discussed.

The paper is prepared as follows. Section 2 explains the IM model. Section 3 presents a novel combined first- and second-order sliding mode control. Section 4 contains a discussion and experimental results. Finally, section 5 presents the conclusion.

2. MODEL DESCRIPTION OF INDUCTION MOTOR WITH FIELD ORIENTATION

The vector control concept has become a standard tool for high-performance control of AC motors. The ultimate

[1] Electrical Engineering Department, LSPIE Laboratory, University Batna2, Batna, Algeria.
E-mails: h.benderradji@univ-batna2.dz, samira.benaicha@univ-batna2.dz, y.laamari@univ-batna2.dz

DOI: 10.59277/RRST-EE.2024.69.4.8

objective of vector control is to enable decoupling control of torque and flux like the power of separately excited direct current (DC) motor. The flux vector φ_r is forced on the d-axis of the (d−q) synchronous reference frame of Park [3], $\varphi_{rd} = \varphi_r, \ , \varphi_{rq} = 0$

In this case, the two phase equivalent IM model, with rotor field orientation, is described by the following equations:

$$\dot{x} = f(x) + g(x)V_s. \tag{1}$$

$$f(x) = \begin{bmatrix} f_1(x) \\ f_2(x) \\ f_3(x) \\ f_4(x) \end{bmatrix} = \begin{bmatrix} -\delta\, i_{sd} + \omega_s i_{sq} + \alpha\beta\, \varphi_{rd} \\ -\omega_s i_{sd} - \delta\, i_{sq} - p\beta\, \omega\, \varphi_{rd} \\ \alpha M\, i_{sd} - \alpha\, \varphi_{rd} \\ \mu\varphi_{rd}\, i_{sq} - \frac{F}{J}\omega - \frac{T_L}{J} \end{bmatrix}$$

$$g(x) = \begin{bmatrix} b & 0 & 0 & 0 \\ 0 & b & 0 & 0 \end{bmatrix}^T = \begin{bmatrix} g_1(x) & 0 & 0 & 0 \\ 0 & g_2(x) & 0 & 0 \end{bmatrix}^T,$$

$x = [i_{sd}\ \ i_{sq}\ \ \varphi_{rd}\ \ \omega]^T$.

For simplicity, we define the following variables:

$$\sigma = 1 - \frac{M^2}{L_s L_r}, \qquad b = \frac{1}{\sigma L_s}\ , \quad T_r = \frac{L_r}{R_r},$$

$$\alpha = \frac{1}{T_r}, \qquad \beta = \frac{M}{\sigma\, L_s L_r}, \qquad \mu = \frac{pM}{J\, L_r}, \quad \delta = \frac{M^2 R_r}{\sigma L_s L_r^2} + \frac{R_s}{\sigma L_s}.$$

where φ_{rd} is the rotor flux, and (i_{sd}, i_{sq}) are the stator currents. The control vector is defined by $V_s = [V_{sd},\ V_{sq}\ ]^T$, and T_L is the load torque, ω is the mechanical frequency of the electrical rotor speed, σ is the total leakage factor. R_s and R_r denote stator and rotor resistance, L_s and L_r are stator and rotor inductance, M is mutual inductance, p is the number of pole pairs, J is the moment of inertia, and F is the friction coefficient.

3. NOVEL COMBINED FIRST AND SECOND-ORDER SLIDING MODE CONTROL

3.1 PROBLEM FORMULATION

The proposed method's objective is to control the rotor speed and the square of the rotor flux separately. The control is based on the employing of two sliding surfaces "S" and " Γ". To apply our control technique, we need to choose two sliding surfaces S and Γ as follows:

The first sliding surface S:

$$S = \begin{bmatrix} S_\omega \\ S_\phi \end{bmatrix} = \begin{bmatrix} \omega_{ref} - \omega \\ \phi_{ref} - \phi \end{bmatrix}. \tag{2}$$

The second sliding surface Γ is [16]:

$$\Gamma = \dot{S} + k|S|sng(S), \tag{3}$$

where $\phi = \varphi_{rd}^2$ and ω_{ref}, ϕ_{ref} are the desired speed and square of the rotor flux references signals with: $\Gamma = \begin{bmatrix} \Gamma_\omega \\ \Gamma_\phi \end{bmatrix}$, $\mathbf{k} = \begin{bmatrix} k_\omega & 0 \\ 0 & k_\phi \end{bmatrix}$, $k_\omega,\ k_\phi > 0$.

The first surface is dependent on the convergence of the second. The system's state transits from the first surface, S to the second surface Γ , and arrives at the origin in finite time.

At first, the system states ω and ϕ will converge, in finite time, to the reference values when they are kept on the sliding surface $\Gamma = 0$ then: $\dot{S} + k|S|sng(S) = 0$. We obtain:

$$\dot{S} = -\mathbf{k}|S|sng(S) \ \rightarrow \ \dot{S} = -kS. \tag{4}$$

Equation (4) ensures the states of speed and the square of rotor flux will exponentially converge to the reference values when they are kept on the sliding surface $S = 0$

Next, the control law is designed for the second-order sliding-mode which drives the state variables to the sliding surface $\Gamma = 0, \dot{\Gamma} = 0$, converging to the zero point along it.

When $\dot{\Gamma} = 0$, we can write:

$$\ddot{S} + \mathbf{k}\dot{S} = 0, \tag{5}$$

we obtain $\ddot{S} = -k\dot{S}$.

In this case, the trajectories are characterized by second-order sliding mode around the origin of a sliding variable.

3.1.1. CONTROL LAW

The derivative of the sliding manifold given by (3) is:

$$\dot{\Gamma} = \ddot{S} + \mathbf{k}\dot{S}. \tag{6}$$

To design the control law, the reaching law is chosen as:

$$\dot{\Gamma} = -\lambda.\, sng(\Gamma). \tag{7}$$

$\lambda = \begin{bmatrix} \lambda_\omega & 0 \\ 0 & \lambda_\phi \end{bmatrix}$, which the constants $\lambda_\omega, \lambda_\phi > 0$. Substitute (3) and (6) into (7), and we can write:

$$\ddot{S} + k\dot{S} = -\lambda.\, sng(\dot{S} + k|S|sng(S)),$$

$$\ddot{S} = -\lambda.\, sng(\dot{S} + k|S|sng(S) - k\dot{S} \tag{8}$$

Hence, the dynamic of first sliding surface S:

$$\begin{aligned} \dot{S}_\omega &= \dot{\omega}_{ref} - \mu\, \varphi_{rd} i_{sq} + \frac{T_L}{J} \\ \dot{S}_\phi &= \dot{\phi}_{ref} + 2\alpha\phi - 2\alpha M\, \varphi_{rd} \end{aligned} \tag{9}$$

The second derivatives of sliding surface S:

$$\begin{aligned} \ddot{S}_\omega &= h_1(x) + D_1(x)V_s \\ \ddot{S}_\phi &= h_2(x) + D_2(x)V_s \end{aligned} \tag{10}$$

where:

$$\begin{aligned} h_1(x) &= \ddot{\omega}_{ref} - \mu\left[\alpha M i_{sd} i_{sq} - (\alpha + \delta)\varphi_{rd} i_{sq} - \omega_s \varphi_{rd} i_{sd} - \beta p \omega \phi\right] + \frac{\dot{T}_L}{J} \\ h_2(x) &= \ddot{\phi}_{ref} - 2\alpha M\left[\alpha M i_{sd}^2 - (3\alpha + \delta)\varphi_{rd} i_{sd} + \omega_s \varphi_{rd} i_{sq}\right] + 2\alpha^2(\beta M + 2) \\ D_1(x) &= -\mu b \varphi_{rd} \\ D_2(x) &= 2\alpha M b \varphi_{rd} \end{aligned}$$

Equation (10) can take the following form:

$$\ddot{S} = h(x) + D(x)\, V_s\,, \tag{11}$$

where: $D(x) = \begin{bmatrix} 0 & D_1(x) \\ D_2(x) & 0 \end{bmatrix}$, $h(x) = \begin{bmatrix} h_1(x) \\ h_2(x) \end{bmatrix}$

By replacing (11) with (5), the second-order sliding mode control law of the system (1) is given as:

$$V_s = \begin{bmatrix} V_{sd} \\ V_{sq} \end{bmatrix} = -D(x)^{-1}\left(\begin{bmatrix} h_1(x) \\ h_2(x) \end{bmatrix} + \begin{bmatrix} \lambda_\omega sgn\left(\dot{S}_\omega + k_\omega |S_\omega| sng(S_\omega)\right) + k_\omega \dot{S}_\omega \\ \lambda_\phi sgn\left(\dot{S}_\phi + k_\phi |S_\phi| sng(S_\phi)\right) + k_\phi \dot{S}_\phi \end{bmatrix}\right) \tag{12}$$

The inverse D^{-1} exists for all time. $h_1(x)$ and $h_2(x)$ must satisfy: $|h_1(x)| < C_0, |h_2(x)| < C_1$, which C_0 and C_1 are the positive constants.

The algorithm's convergence with a prescribed convergence law differs; it's a smooth transition between two sliding modes. This technique can be considered as a

combination of two sliding mode regimes. The first is a classical sliding mode, reached when the surface $\Gamma = 0$. At this time, the system can leave the original surface $\dot{S} = -k|S|sgn(S)$ towards a second-order sliding mode with $\dot{\Gamma} = 0$. When the trajectory approaches the second-order sliding mode, set $\dot{S} = S = 0$, which will be guaranteed, hence the existence of a second-order sliding mode.

To guarantee the global stability of the proposed sliding-mode control system, the sliding-mode controller should satisfy Lyapunov's stability theory [3]. The Lyapunov's positive function is selected as:

$$V = \frac{1}{2}\Gamma^T\Gamma \quad (13)$$

The sliding mode is obtained provided that the Lyapunov attractivity relation is less than zero, *i.e.*, $\dot{V} = \dot{\Gamma}^T\Gamma < 0$.

By replacing (11) into (6) the derivative of V is:

$$\dot{V} = (h(x) + D(x)V_s + k\dot{S})(\dot{S} + k|S|\,sgn(S)). \quad (14)$$

Substituting (12) into (14), the derivative of Lyapunov function V becomes:

$$\dot{V} = -\lambda_\omega|\dot{S}_\omega + k_\omega|S_\omega|sng(S_\omega)| - \lambda_\phi|\dot{S}_\phi + k_\phi|S_\phi|sng(S_\phi)| < 0. \quad (15)$$

With the developed nonlinear sliding-mode controller (12) the reaching Lyapunov function condition $\dot{V} < 0$ is satisfied, and the controlled system will be stabilized.

Remark: From the above control law of eq. (12), implementing these algorithms requires the load torque and rotor flux estimations since stator currents, voltages, and rotor speed are available by measures. The rotor flux is estimated by a 3rd equation of system (1). A simple estimated rotor flux $\hat{\varphi}_r$ is given by the following equation:

$$\hat{\varphi}_r = \frac{M}{T_r s+1} i_{sd} \quad (16)$$

with: $\hat{\phi}_r = \hat{\varphi}_r{}^2$, and s the Laplace's operator.

The estimated load torque can be easily obtained using the motor model's mechanical equation, estimated rotor fluxes, and measured stator currents.

4. EXPERIMENTAL SETUP

The proposed control has been implemented on an experimental setup, which consists of a Dspace card DS1104 with a TMS320F240 slave processor and an ADC interface board CP1104 (Fig.1). A three-phase pulse width modulation (PWM) inverter (Fig. 2) is connected to DC bus voltage, with a switching frequency of 10 kHz. The experimental system has analog inputs, encoder inputs, and PWM output channels.

Tests and results are conducted in the L.T.I laboratory at the University of Picardie Jules Verne, Soissons, France.

(a)

(b)

Fig. 1 – (a) Graphical user interface, (b) Real-time visualization on Simulink/Dspace.

(a)

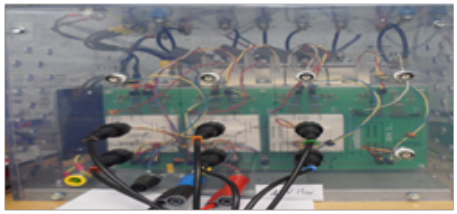

(b)

Fig. 2 – (a) Darlington assembly to supply the drivers with 15 V, (b) PWM Inverter.

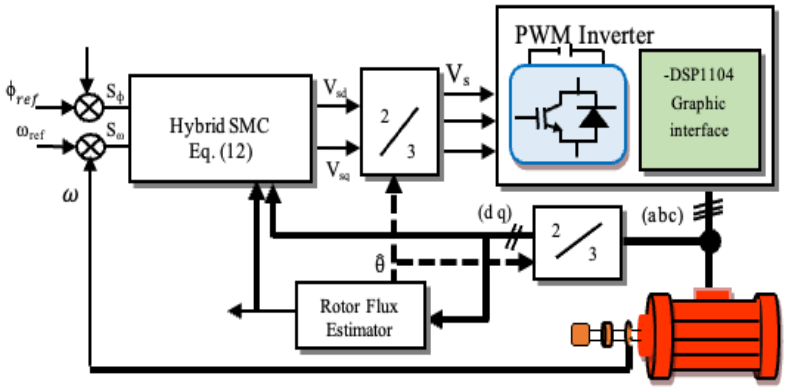

Fig. 3 – Block diagram of the proposed SMC of induction motor.

The control program is written in MATLAB/Simulink real-time interface with a sampling time of 10^{-4} s. Figure 3 depicts the control system for IM's configuration. The induction motor parameters are listed in Table 1.

Table 1.
Induction Motor Parameters

Nominal rate power	1.5 kW	R_r	4. 2 Ω
Nominal rotor speed	1440 rpm	R_s	5.72 Ω
Nominal Voltage	220/380 V	M	0.4402 H
Rated load	10 Nm	L_s, L_r	0.462 H
Number of pole pairs	2	J	0.0049 kg.m^2
		F	0.003 SI

It is assumed that all the parameters are known and constant except for the rotor time constant T_r which will change during the motor operating

4.1. DISCUSSION AND EXPERIMENTAL RESULTS

The motor is required to track the reference speed and square of the rotor flux. Some experimental results are provided here to verify the effectiveness of the proposed method. The reference flux is set to 0.7 Wb, and the load torque () is applied throughout the simulation.

Several tests have been performed to prove the proposed sliding mode approach's performance and robustness, and the results are given in the following figures.

First, we test the speed evolution of the system, given in Fig.4, and show the disturbance rejection. The induction motor is operated from 50 rad/s to 140 rad/s under no load, then a load torque of 7 Nm is applied at t =3 s, and afterward, at t = 9 s, the motor is decelerated to 10 rad/s. The rated load is removed at t =13 s. We can see the rotor flux and speed tracking are very good with a well rejection of the load torque. The stator current in the rotating reference frame (i_{sd}, i_{sq}), and the control vector (Stator voltage V_{sd}, V_{sq}) is used to confirm that the decoupling control is perfect. Also, we note that the chattering in the stator current waveform isa is very weak. In this test, the control performances are very satisfactory.

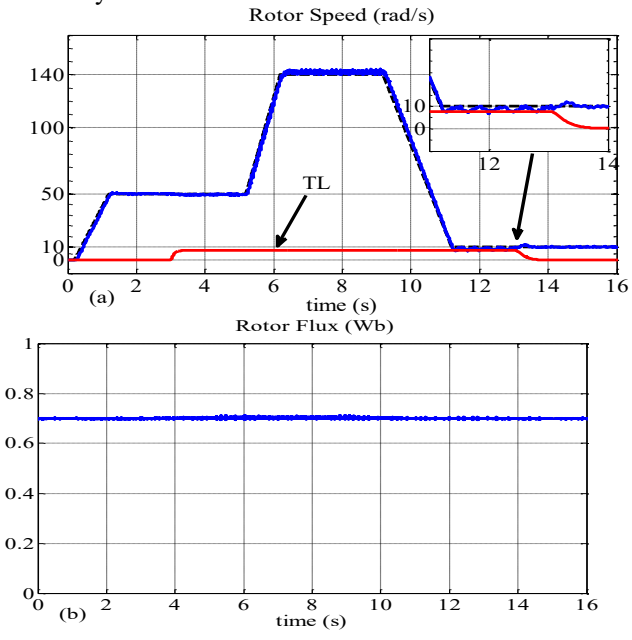

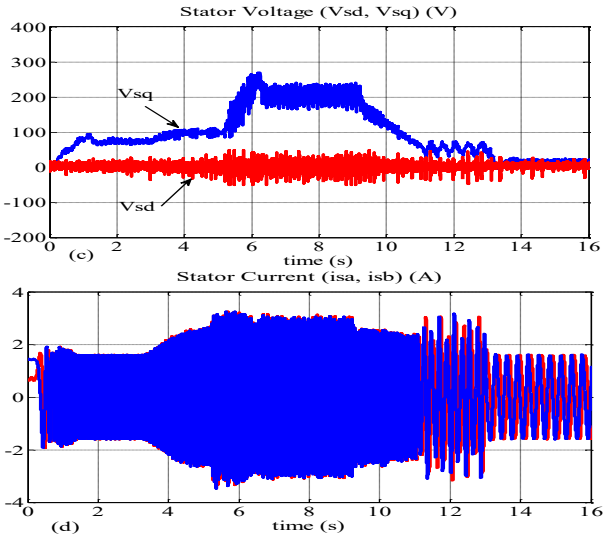

Fig. 4 – Experimental dynamic responses of rotor speed variation under load torque T_L=7 Nm: (a) Rotor speed, (b) Rotor flux, (c) Stator voltage (V_{sd},V_{sq}), (d) Stator current i_{sa}..

Another reference trajectory of rotor flux is tested, as shown in Fig. 5. The rotor flux varies from 0.7 Wb to 0.9 Wb and then decreases to 0.6 Wb. The speed tracking is well maintained, and the reject of the load torque is achieved.

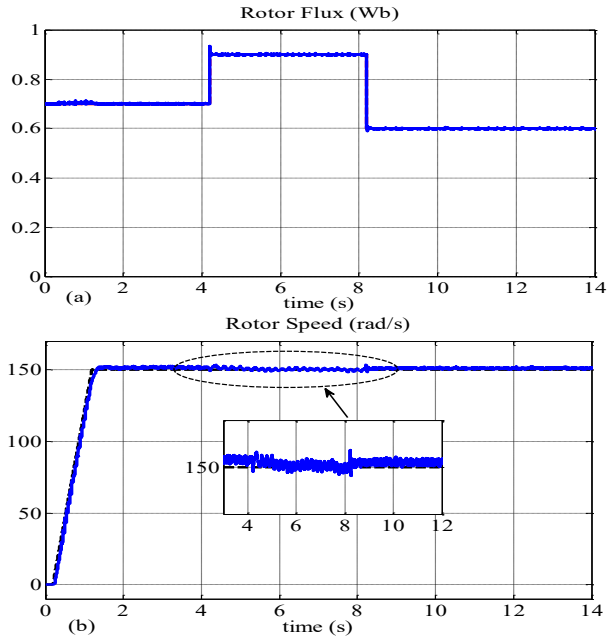

Fig. 5 – Experimental responses of rotor flux variation under load torque T_L= 7 Nm: (a) Rotor flux, (b) Rotor speed.

A last test was performed to validate and evaluate system performance and robustness against the parameters variation. The results reported in Fig.6 illustrate the robustness of the proposed control under increasing in inverse of rotor time constant $1/T_r$, with the presence of load torque at t = 4.2 s. The motor is started with its nominal rotor time constant, then, $1/T_r$, it is suddenly set to +100% variation at t = 8.2 s and eliminated at 12.2 s. The rejection of load torque is very efficient, and a perfect rotor flux orientation on the d-axis of the synchronous reference frame is noted. Thus, good speed regulation and no appreciable variations occur when the torque increases and there is no considerable chattering.

Figure 7 shows the convergence of the speed and flux sliding manifold to zero. Experimental results validate the effectiveness of the proposed technique.

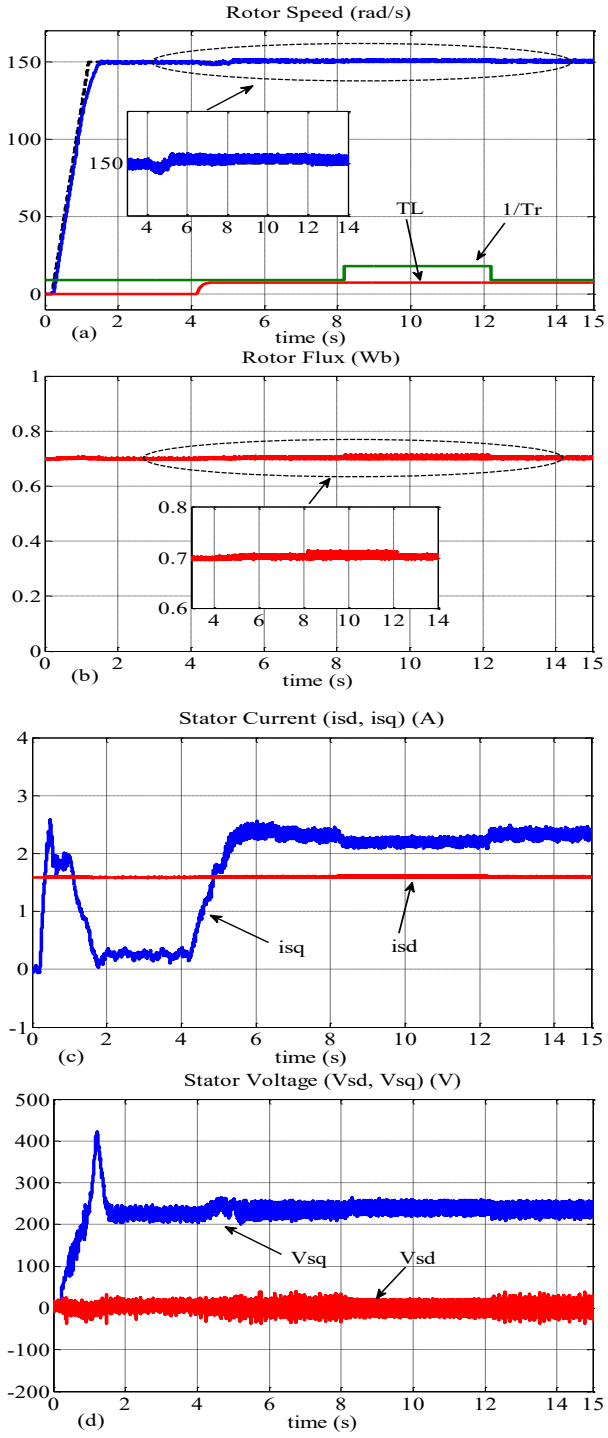

Fig. 6 – Experimental dynamic responses with T_L=7 Nm and 100% 1/Tr variation. (a) Rotor speed, (b) Rotor flux, (c) Stator current (i_{sd}, i_{sq}), (d) Control vector components (V_{sd}, V_{sq}).

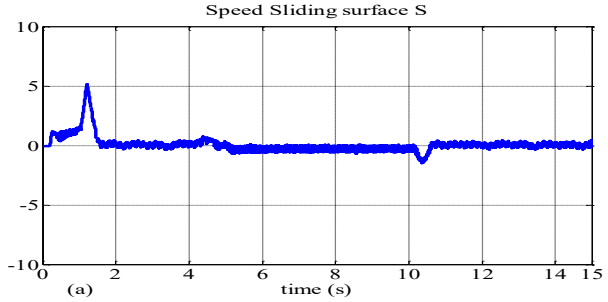

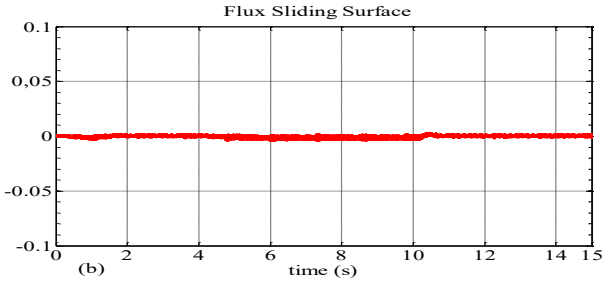

Fig. 7 – Responses of sliding mode surfaces: Rotor speed surface S_Ω., Rotor Flux surface S_ϕ.

5. CONCLUSION

It is concluded from the experimental results that this study has successfully demonstrated the design and implementation of a new sliding mode induction motor control. The developed sliding-mode control law combines first- and second-order sliding-mode techniques using two sliding surfaces. At the same time, the selected sliding surfaces can allow a smooth transition between the two regimes. The proposed approach preserves the merits of classic sliding mode, realizes the merits given by second-order sliding mode, and demonstrates excellent performance and stability under rotor time constant variation, external load disturbances, and speed tracking with negligible chattering. Experimental results are satisfactory, the required performance and robustness are achieved, and the validity of the proposed approach is proved.

Received on 12 July 2024

REFERENCES

1. V.I. Utkin, *Sliding mode control design principles and applications to electric drives*, IEEE Trans on Industrial Electronics, **40**, *1,* pp. 23–36 (1993).
2. V.I. Utkin, J. Guldner, J. Shi, *Sliding mode control in electromechanical systems*, Pub. Boca Raton. 2nd edition 2017. Taylor-Francis Group (2017).
3. O. Barambones, A. Garrido, F. Maseda, *Integral sliding-mode controller for induction motor based on field-oriented control theory*, IET Control Theory Appl., **1**, pp. 786–794 (2007).
4. R. Rai, S. Shukla, B. Singh, *Sensorless field oriented SMCC based integral sliding mode for solar PV based induction motor drive for water pumping*, IEEE Trans. Ind. Appl., **56**, pp. 5056–5064, (2020).
5. A. Devanshu, M. Singhand, N. Kumar, *Sliding mode control of induction motor drive based on feedback linearization*, IETE Journal of Research, **66**, *2*, pp. 256–269 (2020).
6. L. Gou, C. Wang, M. Zhou, X. You, *Integral sliding mode control for starting speed sensorless controlled induction motor in the rotating condition*, IEEE Transactions on Power Electronics, **35**, *4*, pp. 4105–4116 (2019).
7. S.L. Yadav, S.S. Karvekar, *Design of integral sliding mode controller for speed control of induction motor*, In: 2022 2nd International Conference on Intelligent Technologies (CONIT), IEEE, pp. 1–6, (2022).
8. P.J. Shaija, A.E. Daniel, *Robust sliding mode control strategy applied to IFOC induction motor drive*, In: 2021 Fourth International Conference on Electrical, Computer and Communication Technologies (ICECCT), IEEE, pp. 1–6 (2021).
9. C.M. Oliveira, M.L. Aguiar, J.R. Monteiro et al, *Vector control of induction motor using an integral sliding mode controller with anti-windup*, J. Control Autom.. Electr. Syst., **27**, pp. 169–178 (2016).
10. M.S. Mousavi, S.A. Davari, V. Nekoukar et al, *Integral sliding mode observer-based ultra-local model for finite-set model predictive current control of induction motor*. IEEE J. Emerg. Sel. Top. Power Electron., 10, pp. 2912–2922, (2021).
11. M.H. Park, K.S. Kim, *Chattering reduction in the position control of induction motor using the sliding mode*, IEEE Trans on Power Electronics, **6**, *3*, pp. 317–325 (1991).
12. A. Bennassar, S. Banerjee, M. Jamma et al, *Real time high performance of sliding mode-controlled induction motor drives*, Procedia computer science, **132**, pp. 971–982, (2018).

13. D. Zellouma, Y. Bekakra, H. Benbouhenni, *Robust synergetic-sliding mode-based-backstepping control of induction motor with MRAS technique*, Energy Reports, **10**, pp. 3665–3680 (2023).
14. I. Bendaas, F. Naceri, *A new method to minimize the chattering phenomenon in sliding mode control based on intelligent control for induction motor drives*, Serbian Journal of Electrical Engineering SJEE, 10(2), pp. 231–246, (2013).
15. A. Levant, *Sliding order and sliding accuracy in sliding mode control*, International Journal of Control, **58**, *6*, pp. 1247-1263 (1993).
16. A. Levant, *Principles of 2-sliding mode design*, Automatica, Elsevier Science, **43**, pp. 576–586, (2007).
17. T. Floquet, J.P. Barbot, W. Perruquetti, *Second order sliding mode control for induction motor*, 39th IEEE Conf. on Decision and Control, Sydney, Australia**, 2**, pp. 1691–1696, (2000).
18. J. Mishra, L. Wang, Y. Zhu et al, *A novel mixed cascade finite-time switching control design for induction motor*. IEEE Trans. Ind. Electron., **66**, pp. 1172–1181 (2018).
19. F. Yeshiwas, S. Dereje, *Fractional order sliding mode speed control of feedback linearized induction motor*, Power Electronics and Drives, **5**, *1*, pp. 109–122 (2020)
20. M. Zand, M.A. Nasab, M. Khoobani et al., *Robust speed control for induction motor drives using STSM control*, 12th Power Electronics, Drive Systems, and Technologies Conference (PEDSTC). IEEE, pp. 1–6 (2021).
21. B. Wang, T. Wang, Y. Yu et al., *Second-order terminal sliding-mode speed controller for induction motor drives with nonlinear control Gain*, IEEE Transactions on Industrial Electronics, **70**, *11*, pp. 10923–10934 (2022).